


FULL PAPER

Open Access



# Migration of earthquakes with a small stress drop in the Tanzawa Mountains, Japan

Takuji Yamada<sup>1\*</sup> , Yohei Yukutake<sup>2</sup>, Toshiko Terakawa<sup>3</sup> and Ryuta Arai<sup>4</sup>

## Abstract

A cluster of earthquake activity took place beneath the Tanzawa Mountains at a depth of 20 km during the end of January 2012. The activity began at 22:39 UT on January 27 and included 78 earthquakes with magnitudes of 2.0 and greater within the span of 50 h. Five of them had magnitudes greater than 4.0, and the largest one was a M5.4 earthquake. We relocated the hypocenters by using the double-difference method and characterized their migrations away from the first earthquake of the cluster activity. The migration was consistent with fluid diffusion and had a similar speed to that of non-volcanic tremors and of induced earthquakes caused by water-injection experiments. We then analyzed stress drops for 16 earthquakes of M3.5 and greater that occurred from July 2003 to June 2012 in the area of the cluster activity. Earthquakes that occurred before and after the cluster activity had typical and stable values of stress drop. This is consistent with structural studies indicating the existence of little fluid in the region. In contrast, the cluster activity included earthquakes with significantly small stress drops. The leading hypothesis is that the cluster activity was associated with a decrease in the shear strength due to an increase in pore pressure, and this can explain both the migration of hypocenters and the small stress drops associated with the cluster activity. This hypothesis is also supported by the fact that earthquakes before and after the cluster activity had similar values of stress drop, thus suggesting that the activity was triggered by a different mechanism from the other earthquakes in the same region. The most plausible explanation is that there is a little fluid in the closed system beneath the Tanzawa Mountains that is undetectable by structural observations.

**Keywords:** Migration of hypocenters, Stress drop, Cluster activity, Fluid, Tanzawa Mountains

## Background

A cluster of earthquake activity took place in 2012 beneath the Tanzawa Mountains in Japan at a depth of 20 km. In order to investigate what caused the activity, we relocated the hypocenters and estimated stress drops of the earthquakes involved in the cluster activity as well as the values of other earthquakes before and after the activity in the same region. We characterized the migration of the hypocenters and found that earthquakes during the cluster activity included earthquakes with smaller values of stress drop. Herein, we discuss possible causes of the activity, as well as relationships to the tectonic characteristics and the velocity structure of the source region.

## Seismicity and tectonics in the Tanzawa Mountains

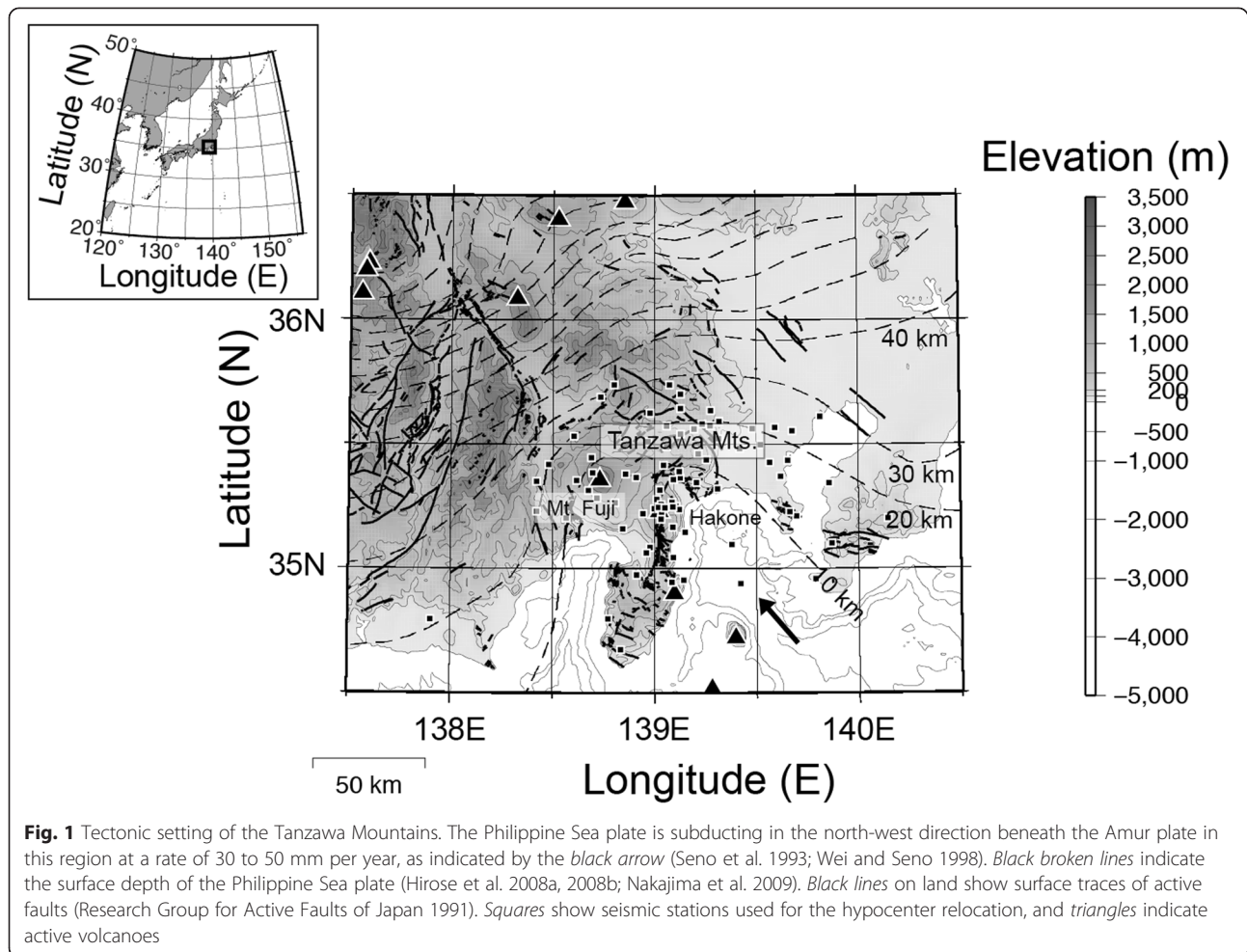
The Tanzawa Mountains in Japan is located in the Izu-Honshu collision zone, where the Izu-Bonin arc on the Philippine Sea plate has been colliding with Honshu Island on the Okhotsk and Amur plates (Fig. 1; Arai and Iwasaki 2014, 2015). Several tectonic faults have developed in this region, and the seismicity is very high (Fig. 2). Most earthquakes in the region have reverse-faulting focal mechanisms, which is consistent with the stress condition due to the collision (Terakawa and Matsu'ura 2010). In addition, the 1923 Kanto earthquake  $M_W$  7.9 ruptured the interface on the subducting Philippine Sea plate and the northwestern tip of the rupture was located beneath the Tanzawa Mountains (Kobayashi and Koketsu 2005).

Yukutake et al. (2012) investigated the detailed distribution of hypocenters and focal mechanisms beneath the Tanzawa Mountains. Focal mechanisms of earthquakes associated with the cluster activity in January

\* Correspondence: takuji.yamada.t9sci@vc.ibaraki.ac.jp

<sup>1</sup>Department of Earth Sciences, Faculty of Science, Ibaraki University, Mito, Ibaraki, Japan

Full list of author information is available at the end of the article



2012 were consistent with the results of Yukutake et al. (2012), as well as the tectonic stress field (Terakawa and Matsu'ura 2010). Figure 3 shows hypocenters of earthquakes with magnitudes of 2.0 and greater in the Tanzawa Mountains from 2000 to 2012 that were detected by the Japan Meteorological Agency (JMA). The data indicate that the cluster activity in January 2012 was unique from the viewpoint of earthquake magnitudes in that the activity included several earthquakes with magnitudes around 5. Figure 3 also shows that the hypocenters of earthquakes involved in the cluster activity were located within areas with constantly high seismicity.

In this paper, we focused on the January 2012 cluster activity in the area with constantly high seismicity and investigated the migration and stress drops of earthquakes.

#### Studies on seismicity and stress drop

Seismicity and its spatiotemporal change provide us with information about the physical conditions in seismogenic regions. Dieterich (1994) related the rate of

earthquake generation to the applied stressing history through the rate- and state-dependent friction law and derived general formula for estimating the stressing history from the observed seismicity. Toda et al. (2002) applied the formula to the 2000 Izu Islands earthquake swarm and estimated the stressing rate. They concluded that the obtained stressing rate was consistent with magma intrusion into a vertical dyke rather than ground water diffusion. These results were mainly obtained from the temporal change of seismicity. Studies on spatial change of seismicity include the following papers. Ando and Imanishi (2011) investigated the seismicity between the  $M_W$  7.3 earthquake on March 9, 2011 (foreshock) and the  $M_W$  9.0 Tohoku-oki earthquake on March 11, 2011. They found that hypocenters appeared to migrate toward the  $M_W$  9.0 earthquake and proposed the possibility that these earthquakes were triggered by diffusional propagation of afterslip from the  $M_W$  7.3 foreshock. Referring to the hypocenters determined by the JMA, the foreshock activity of the 2011 Tohoku-oki earthquake may have started at least in the middle of February 2011 (Hirose et al. 2011). Kato et al. (2012) applied a matched-filter

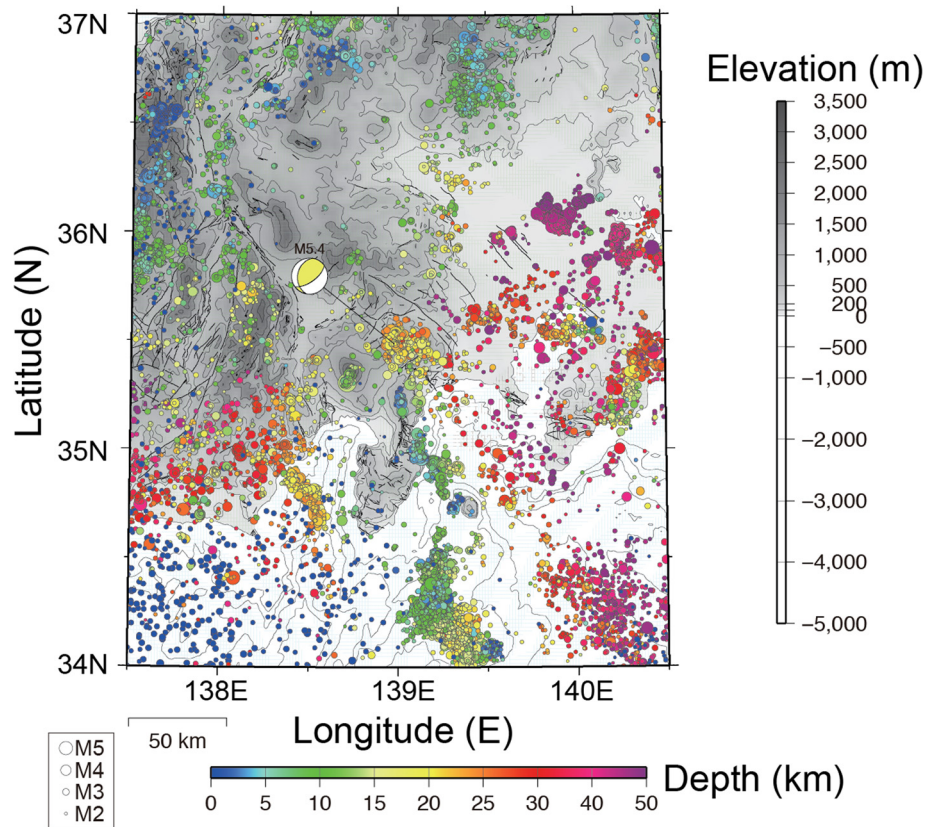


**Fig. 2** Seismicity in and around the Tanzawa Mountains from 2000 to 2012 for  $M \geq 2$  earthquakes that were detected by the Japan Meteorological Agency. Earthquakes shallower than 50 km are plotted with a color scale indicating the hypocentral depth. The focal mechanism of the largest earthquake (M5.4) of the cluster activity in January 2012 is also plotted

technique (e.g., Shelly et al. 2007) for continuous seismograms and found more than 1000 undetected earthquakes between February 13 and March 11, 2011, when the 2011  $M_W$  9.0 Tohoku-oki earthquake took place. Based on a space-time diagram of all the detected earthquakes, they identified two distinct sequences of earthquake migration toward the hypocenter of the 2011  $M_W$  9.0 Tohoku-oki earthquake in the direction parallel to the trench axis; one was from the middle to the end of February and the other occurred between March 9 and 11, similar to the results of Ando and Imanishi (2011). They concluded that it was most plausible that these migration sequences were due to the propagation of slow slips.

The stress drop is another important source parameter that is indicative of the difference between the initial and residual stress levels. Stress drops of small and large earthquakes have been estimated to investigate the self-similarity of earthquakes (e.g., Abercrombie 1995; Kanamori and Anderson 1975; Prieto et al. 2004; Yamada et al. 2007). Recently, Yoshimitsu et al. (2014) investigated acoustic emission (AE) events of a rock fracture experiment under seismogenic pressure

conditions and pointed out that the AE events with magnitudes down to  $-8$  satisfied the proportionality between the seismic moment and the corner frequency to the third power, or the constant stress drop. Another aspect of the stress drop analysis is the spatiotemporal heterogeneity of stress and strength. The initial stress should be equal to the strength at the hypocenter, where the rupture starts, so stress drops of small earthquakes can be a good indicator for the spatial distribution of the difference between the strength and the dynamic stress level (Yamada et al. 2010).

Allmann and Shearer (2007) analyzed stress drops of small earthquakes near Parkfield, California, and investigated the relationships of their spatial and temporal variations to the source area of the 2004 Parkfield earthquake. They found that stress drops of small earthquakes around the 2004 Parkfield earthquake had large values. At an even finer scale, Yamada et al. (2010) analyzed stress drops of small earthquakes that occurred on the fault plane of the Kiholo Bay earthquake ( $M_W$  6.7) and compared the values to the slip distribution of the earthquake. They found that small earthquakes around large slip patches of the main shock were likely to have

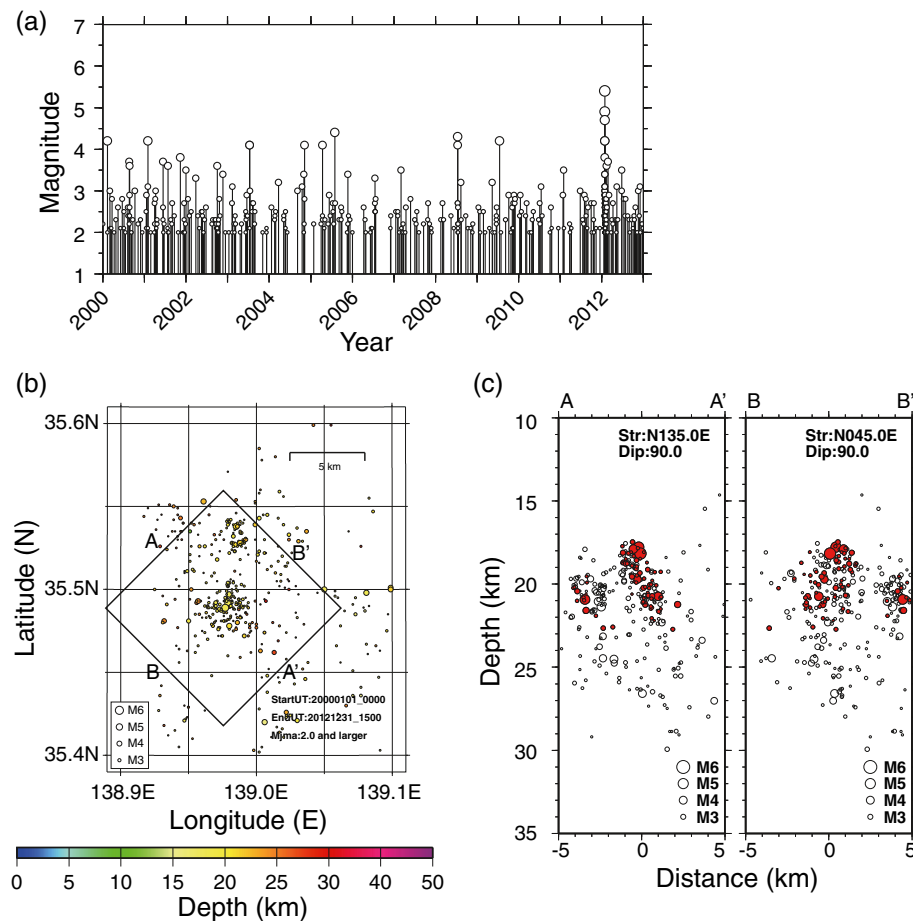


**Fig. 3** **a** Seismicity in the Tanzawa Mountains from 2000 to 2012 ( $M \geq 2$ ) as a function of time. Earthquakes with latitudes from  $35.4^\circ$  N to  $35.6^\circ$  N, longitudes from  $138.9^\circ$  E to  $139.1^\circ$  E, and depths shallower than 50 km are plotted. **b** Map view of the seismicity. The size and color of the symbols indicate the magnitude and depth of the earthquakes, respectively. Cross sections of the seismicity in the square are shown in **(c)**. **c** Cross section of the seismicity with strikes of  $N135^\circ$  E and  $N45^\circ$  E. Red symbols show hypocenters of earthquakes that occurred within 50 h after the first earthquake of the cluster activity at 22:39 UT on January 27, 2012

larger stress drops. They concluded that the spatial pattern of the stress drop reflects coherent variations in the difference between the strength and the residual stress level. Oth (2013) estimated stress drops of earthquakes in Japan and concluded that the values were strongly correlated with heat flow variations, thus suggesting that lower shear strengths are present in the geothermal area.

Most previous studies have suggested that earthquakes associated with water-injection experiments and reservoirs have smaller stress drops than natural ones, but this is not always the case. Goertz-Allmann et al. (2011) analyzed stress drops of earthquakes induced by a water-injection experiment into a borehole and obtained a clear increase in the stress drop as a function of distance from the injection point, thus suggesting that the stress drop correlates with pore pressure perturbations due to the injection. Tomic et al. (2009) estimated stress drops of reservoir-induced earthquakes with  $M \leq 2.1$  and

concluded that the values were similar to those of natural earthquakes. They speculated that the reservoir-induced earthquakes they had analyzed were intra-plate earthquakes in the fresh rock and these showed higher stress drops than the values of other fluid-induced earthquakes.

### Data and Methods

In this paper, we analyzed hypocenter migration and stress drops associated with the cluster activity beneath the Tanzawa Mountains in January 2012 and investigated what caused the activity.

### Hypocenter relocation of the cluster activity

A cluster of earthquake activity took place beneath the Tanzawa Mountains at a depth of 20 km during the end of January 2012. The JMA determined the hypocenters of earthquakes with magnitudes down to  $-1$ , which included 78 earthquakes with magnitudes of 2.0 and



greater; these occurred in the area within 50 h after the first M4.9 earthquake struck at 22:39 UT on January 27. Five of them had magnitudes greater than 4.0, and the largest one was a M5.4 earthquake.

We relocated the hypocenters by using the double-difference (DD) relocation method (Waldhauser and Ellsworth 2000) following Yukutake et al. (2012). We first used the one-dimensional velocity structure in the Tanzawa Mountains as estimated by Hiraga (1987) and determined the initial hypocenters for the DD relocation. We also used seismograms at Hi-net stations operated by the National Research Institute for Earth Science and Disaster Prevention, Japan (NIED), as well as station data from the Hot Spring Research Institute of Kanagawa Prefecture, the Univ. of Tokyo, and the JMA. Furthermore, we used data from the seismograph network called MeSO-net (Hirata et al. 2009; Sakai and Hirata 2009), which was developed in 2007 under the “Special Project for Earthquake Disaster Mitigation in the Tokyo Metropolitan Area.” Stations used for the relocation are shown in Fig. 1. We then carried out the DD relocation by using manually picked P- and S-wave arrival times, as well as the differential ones obtained by the waveform cross-correlation analysis. The correlation measurements were conducted by using the velocity waveforms with a time window of 0.75 s and with a band-passed filter from 3 to 20 Hz. We excluded differential arrival time data with normalized cross-correlation coefficients of less than 0.80 from the DD analysis.

We used 54,047 manually picked and 37,301 cross-correlated pairs of differential arrival times for P waves in the hypocenter relocation. For S waves, there were 47,823 and 31,630 pairs of manually picked and cross-correlated data, respectively. By using both the manually picked and cross-correlation data, we relocated 218 earthquakes down to M0.6 (53 earthquakes with  $M \geq 2.0$ ) during the 2 weeks after the first earthquake of the cluster activity on January 27, 2012 at 22:39 UT.

In order to assess the uncertainty of the hypocenter location, we applied the bootstrap resampling method (Shearer 1997; Waldhauser and Ellsworth 2000) to all the relocated earthquakes. Once the hypocenters were relocated, we could obtain the travel-time residuals of P and S waves for each pair of stations. The average values and standard deviations of double-difference residuals were  $4.91 \pm 4.32$  ms and  $6.27 \pm 5.34$  ms for P and S waves, respectively. We then created synthetic data by picking up the residuals randomly and adding them to the synthetic travel-time data. We relocated all the earthquakes by using the synthetic data and investigated shifts in the locations from the hypocenters estimated by the real data set. This procedure was repeated 200 times. The relative location error of hypocenters was defined

as twice the standard deviation ( $2\sigma$ ) for the location shifts from the hypocenters estimated by the real data set. The errors were estimated as 0.022, 0.018, and 0.030 km in the east–west, north–south, and up–down directions, respectively.

### Stress drop analysis

If an earthquake is caused by the dislocation on a circular fault with a radius  $r$ , the static stress drop  $\Delta\sigma$  of an earthquake with seismic moment  $M_0$  can be written, as described in Eshelby (1957), as

$$\Delta\sigma = \frac{7}{16} \frac{M_0}{r^3}. \quad (1)$$

We can calculate the stress drop following Madariaga (1976) as

$$\Delta\sigma_P = \frac{7}{16} M_0 \left( \frac{f_C^P}{0.32V_S} \right)^3, \quad (2)$$

$$\Delta\sigma_S = \frac{7}{16} M_0 \left( \frac{f_C^S}{0.21V_S} \right)^3, \quad (3)$$

where  $f_C^P$  and  $f_C^S$  are corner frequencies of P and S waves, respectively. We will refer to  $\Delta\sigma_P$  and  $\Delta\sigma_S$  in Eqs. (2) and (3) as stress drops in this study. The model of Madariaga (1976) assumes that the rupture speed is 90 % of the shear wave velocity, and this is generally consistent with the rupture speeds of large and small earthquakes (e.g., Imanishi et al. 2004; Ishii et al. 2005; Wald and Heaton 1994; Yamada et al. 2005). Thus, we used the model of Madariaga (1976) for estimating the stress drops of the small earthquakes in this study. We should note that the estimated stress drops by the model of Madariaga (1976) are 5.6 times larger than the values estimated by the model of Brune (1970). To avoid confusion, we emphasize again that we call the values of stress drop calculated by the model of Madariaga (1976) stress drops in this paper.

We analyzed stress drops of 16 earthquakes ( $3.5 \leq M \leq 5.4$ ) that occurred between 2003 and 2012 in the Tanzawa Mountains. Six out of the 16 earthquakes were included in the cluster activity during January 2012. Eight and the remaining two of the 16 earthquakes occurred prior to and after the cluster activity, respectively (Table 1). The detailed procedure used for the analysis was as follows.

We used earthquakes with  $3.0 \leq M \leq 3.2$  closest to analyzed earthquakes as individual empirical Green's functions (EGFs); we deconvolved the waveforms of vertical (P) and two horizontal (S) components with the EGF waveforms at each station by using three moving windows (Imanishi and Ellsworth 2006), namely,  $-0.50$  to  $4.61$  s,  $0.78$  to  $5.89$  s, and  $2.06$  to  $7.17$  s after the P or

**Table 1** Stress drops for the 16 earthquakes that were analyzed in this study

Origin time (UT)		Lat. (N)	Lon. (E)	Dep. (km)	$M_W$	Stress drop (MPa) <sup>a</sup>	
20030711	0523	35.501	139.099	21.1	4.1	102 (3.36–3120)	34.0 (1.63–710)
20030711	1731	35.500	139.099	21.7	4.1	99.1 (6.12–1600)	42.2 (1.31–1360)
20041108	1848	35.490	138.980	26.6	4.1	6.54 (0.317–135)	20.6 (1.33–320)
20050412	0409	35.493	138.957	24.5	4.1	37.7 (12.5–114)	42.3 (1.35–1320)
20050731	0553	35.553	138.961	22.4	4.4	11.6 (6.62–20.5)	50.0 (6.98–358)
20080715	1323	35.528	138.988	21.4	4.3	–	18.8 (6.24–56.9)
20090715	2019	35.420	139.006	15.7	4.2	–	114 (15.4–839)
20110130	2303	35.543	138.944	25.1	3.5	0.787 (0.00383–162)	0.510 (0.00740–35.1)
20120127	2239	35.492	138.979	17.8	4.9	20.4 (1.86–223)	63.6 (8.89–455)
20120127	2243	35.489	138.977	18.2	5.4	8.24 (4.00–17.0)	41.2 (6.40–265)
20120127	2245	35.488	138.973	19.7	3.8	0.215 (0.00333–13.9)	0.202 (0.0189–2.16)
20120127	2246	35.478	138.980	20.8	4.2	2.92 (0.292–29.2)	7.71 (1.86–32.0)
20120127	2304	35.497	138.980	17.9	4.2	1.84 (0.415–8.20)	2.67 (1.07–6.63)
20120129	0746	35.538	138.985	20.9	4.7	–	37.4 (8.15–172)
20120212	0151	35.481	138.950	19.4	3.6	2.92 (0.0606–141)	28.1 (0.624–1260)
20120623	1441	35.492	138.970	18.9	3.5	19.1 (3.96–91.7)	20.0 (0.646–620)

<sup>a</sup>Left and right values show stress drops estimated by P and S waves, respectively. Values in parentheses indicate the ranges for two standard deviations.

S arrivals. Each time window contained 512 data points. It is generally preferable that the analyzed and EGF earthquakes are different in magnitude by more than 1 magnitude unit for estimating a reliable corner frequency. However, the use of smaller earthquakes as Green's functions limits the availability of stations because of the poor signal-to-noise ratio of waveforms. This is why we used earthquakes with  $3.0 \leq M \leq 3.2$  as EGFs. We confirmed that the fit of synthetic spectral ratios to the observed ones was fair and that the estimated corner frequencies would be robust even for earthquakes with  $M$  values smaller than 4.0.

Following Boatwright (1978), we then approximated the deconvolved velocity amplitude spectra  $|\dot{u}_r^C(f)|$  as

$$|\dot{u}_r^C(f)| \approx R_r^C M_{0r}^C \left\{ \frac{1 + (f/f_{0E}^C)^4}{1 + (f/f_{0A}^C)^4} \right\}^{1/2}, \quad (4)$$

where  $R_r^C$  and  $M_{0r}^C$  are ratios of the analyzed and EGF earthquakes on the radiation pattern coefficient and the seismic moment, respectively, and  $C$  indicates the wave types, which are either P or S. The value of  $R_r^C$  is 1 if focal mechanisms and hypocenters of the analyzed and EGF earthquakes are exactly the same. Subscripts  $A$  and  $E$  for the corner frequency  $f_0^C$  indicate the analyzed and EGF earthquakes, respectively. Following Yamada et al. (2007, 2010), we took the logarithm of Eq. (4),

$$\ln |\dot{u}_r^C(f)| \approx g(f; f_{0A}^C, f_{0E}^C), \quad (5)$$

$$g(f; f_{0A}^C, f_{0E}^C) = \ln(R_r^C M_{0r}^C) - \frac{1}{2} \ln \left( 1 + (f/f_{0A}^C)^4 \right) + \frac{1}{2} \ln \left( 1 + (f/f_{0E}^C)^4 \right), \quad (6)$$

and found values of  $R_r^C M_{0r}^C$ ,  $f_{0A}^C$ , and  $f_{0E}^C$  for each station by a grid search that gave the minimum residual

$$\text{res} = \sum_i \frac{[\ln \dot{u}_r^C(f_i) - g(f_i; f_{0A}^C, f_{0E}^C)]^2}{\sigma_i^2}, \quad (7)$$

where  $\sigma_i$  is the standard deviation for each data point calculated in resampling the spectrum. More than five stations were available for all the 16 earthquakes for the estimation of corner frequencies. Figure 4 helps to illustrate the procedures used so far, and it shows S waveforms of an analyzed earthquake and EGF at one station and the deconvolved spectra for three time windows. We finally calculated stress drops from the corner frequencies, assuming that  $M$  is equivalent to the moment magnitude  $M_W$ . We obtained a stress drop for each earthquake as the average value of estimated stress drops at all the stations. Seismic moment  $M_0$  in newton meters (Nm) can be calculated from  $M_W$  by the equation (Hanks and Kanamori 1979):  $\log M_0 = 1.5 M_W + 9.1$ .

## Results

### Hypocenter migration

Figure 5 shows the hypocenters of the cluster activity in January 2012 that were relocated by the double-

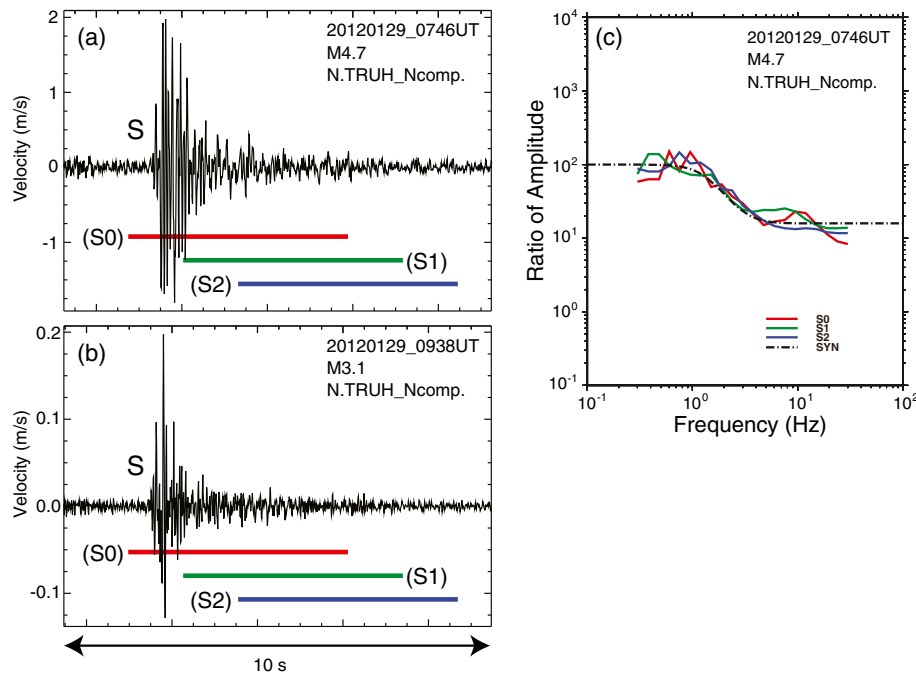


**Fig. 4** S-wave seismograms of (a) M4.7 and (b) M3.1 earthquakes at the station N.TRUH. Color lines indicate the three time windows used in deconvolution, which were (S0)  $-0.50$  to  $4.61$  s, (S1)  $0.78$  to  $5.89$  s, and (S2)  $2.06$  to  $7.17$  s after S arrival. Each time window has 512 data points. **c** Deconvolved spectra with the fitted omega squared model. Color lines are deconvolved source spectra, that is, (a) divided by (b) for the individual three time windows. The black broken line shows the fitted omega squared model

difference relocation method with the waveform cross-correlation (Yukutake et al. 2012) as well as the original ones determined by the JMA. Color indicates the elapsed time of earthquakes from the first earthquake ( $M_W$  4.9). The focal mechanisms of the largest four earthquakes ( $4.4 \leq M_W \leq 5.4$ ) identified by NIED are also shown in Fig. 5. The largest earthquake of the cluster activity ( $M_W$  5.4) occurred 4 min after the first one. We can clearly see that earthquakes of the cluster activity took place on a south-east dipping plane, which is consistent with a nodal plane of the largest earthquake. We also found that the earthquakes showed migration patterns from the first earthquake.

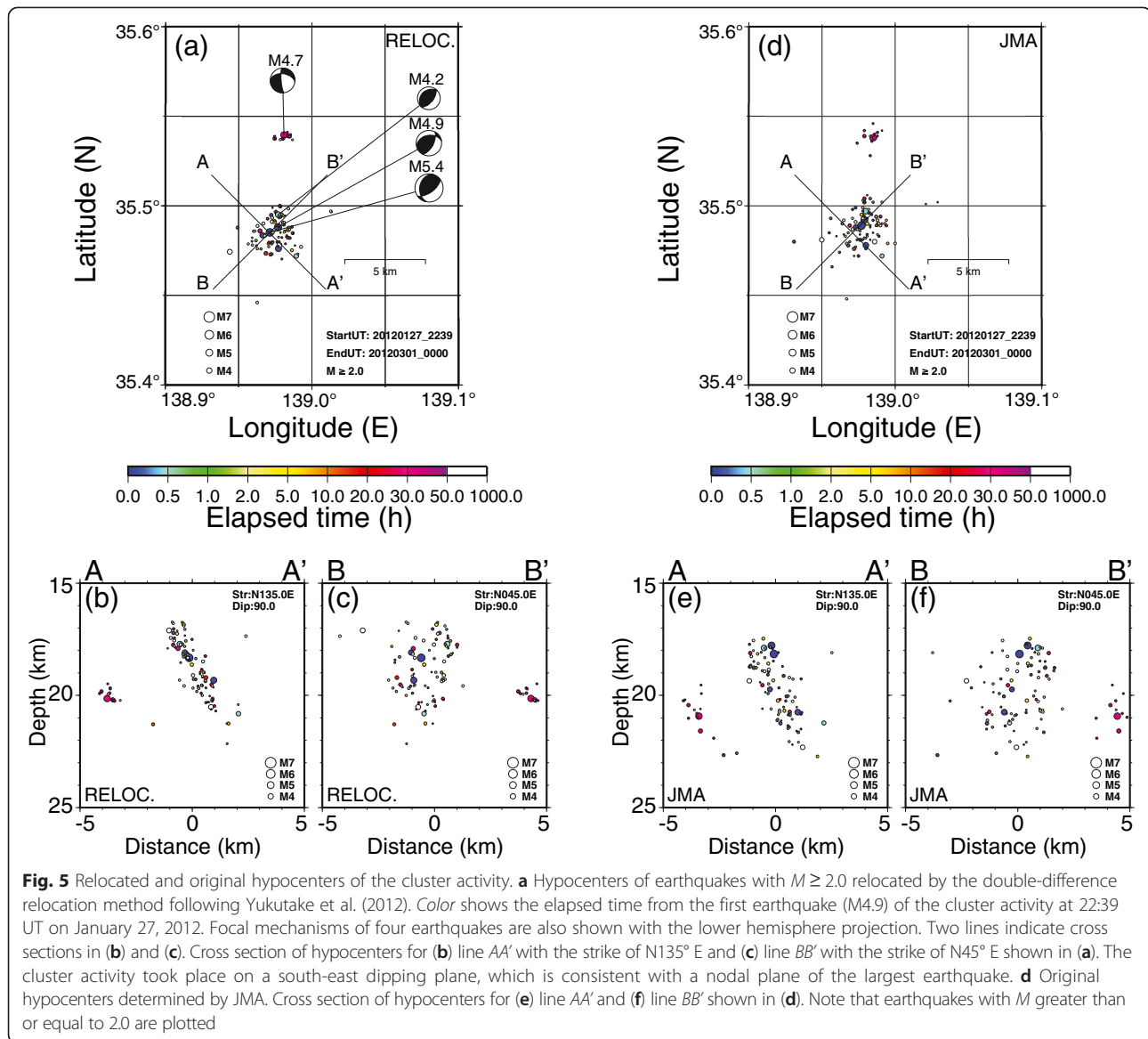
It is true that the width of the south-east dipping “cloud” of relocated hypocenters looks wider than the errors of the hypocenter determinations estimated in “Hypocenter relocation of the cluster activity”. One possibility would be that the errors were underestimated. Another possibility is that the earthquakes took place on a couple of parallel planes (e.g., Naoi et al. 2015). Unfortunately, it is quite difficult to investigate which would be the most plausible explanation from our results.

In order to discuss the hypocenter migration, we plotted the relationship between the elapsed time and the distance from the first earthquake of the cluster activity in Fig. 6. This figure confirms that earthquakes migrated from the first earthquake associated with the cluster

activity. For an elapsed time of less than 1.0 h, the migration followed a parabolic line with a diffusivity  $D$  of  $5.0 \times 10^2 \text{ m}^2 \text{ s}^{-1}$ , which has been defined by Biot (1962) and Shapiro et al. (1997) as

$$r = \sqrt{4\pi Dt}, \quad (8)$$

where  $r$  and  $t$  are the distance and time from the origin, respectively. This value of diffusivity is also consistent with the migration of non-volcanic deep tremors in western Shikoku, south-west Japan (Ide 2010), for which fluid likely plays an important role. Here, we have to note that Ide (2010) reported that the migration followed a curve with a constant diffusion coefficient  $\bar{d}$  of  $10^4 \text{ m}^2 \text{ s}^{-1}$ , which was defined as  $\pi r^2 = \bar{d}t$ , where  $r$  and  $t$  denote the distance and duration of the migration, respectively. If we express the curve with the diffusivity  $D$ , the value is  $2.5 \times 10^2 \text{ m}^2 \text{ s}^{-1}$  and this is of the same order of migration as the first hour of the cluster activity. We can also see that the seismicity for elapsed times larger than an hour shows migrations with rates of 1 to 3 km a day. This is of the same order as the migration rate for water-injection experiments (e.g., Shapiro et al. 1997; Tadokoro et al. 2000) with a diffusivity of  $1.0 \text{ m}^2 \text{ s}^{-1}$ , which is shown as a blue line in Fig. 6. These two features suggest that fluid played an important role in the cluster activity.

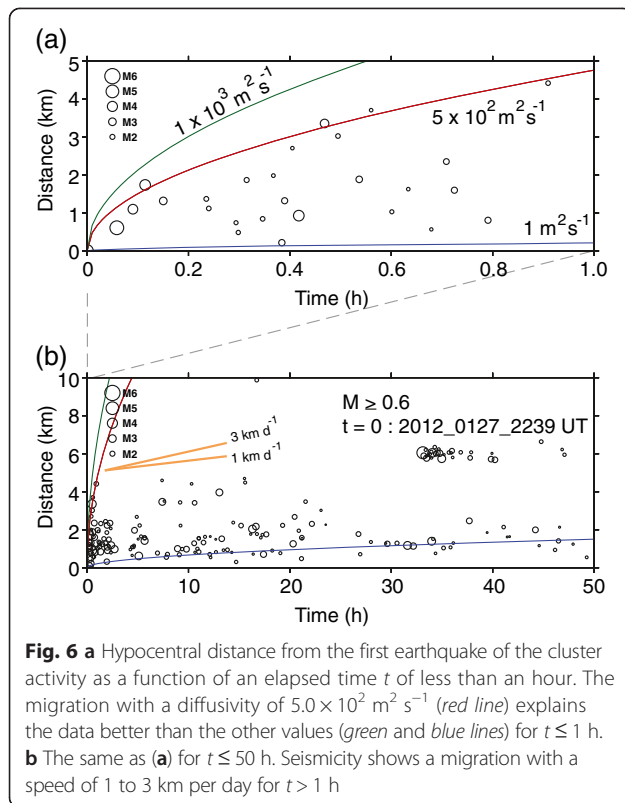


### Small stress drop

Seismic stations used for the stress drop analysis and epicenters of the 16 analyzed earthquakes are shown in Fig. 7. This figure indicates that we had good azimuthal coverage, which is crucial for obtaining reliable values of stress drop estimated from direct waves. Stress drops of the 16 earthquakes are shown in Table 1. Values of stress drop ranged from 0.20 to 114 MPa, and most earthquakes had values around 30 MPa (5.4 MPa if we use the model of Brune (1970)), which is consistent with previous studies on stress drops of earthquakes for a large range of seismic magnitudes (e.g., Abercrombie 1995; Kanamori and Anderson 1975). Values of the stress drop from P waves for three earthquakes could not be calculated because the spectral ratios of P waves for the earthquakes were unavailable as a result of the

limited data on P-wave arrival times for EGF earthquakes. Discrepancy in the values from P and S waves would mainly come from the precision in estimating corner frequencies of P and S waves. Because the stress drop is proportional to the estimated corner frequency to the third power, as seen in Eqs. (2) and (3), uncertainties would be inevitably amplified. Figure 8 shows the values of stress drop as a function of time, with standard deviations for the calculated average values (see “Stress drop analysis”). It is important to emphasize here that estimated values of stress drop showed no temporal change except for the earthquakes involved in the cluster activity, despite the difficulty of the analysis as explained above. We found that three out of the six earthquakes associated with the cluster activity in January 2012 had smaller stress drops by an order of magnitude than the

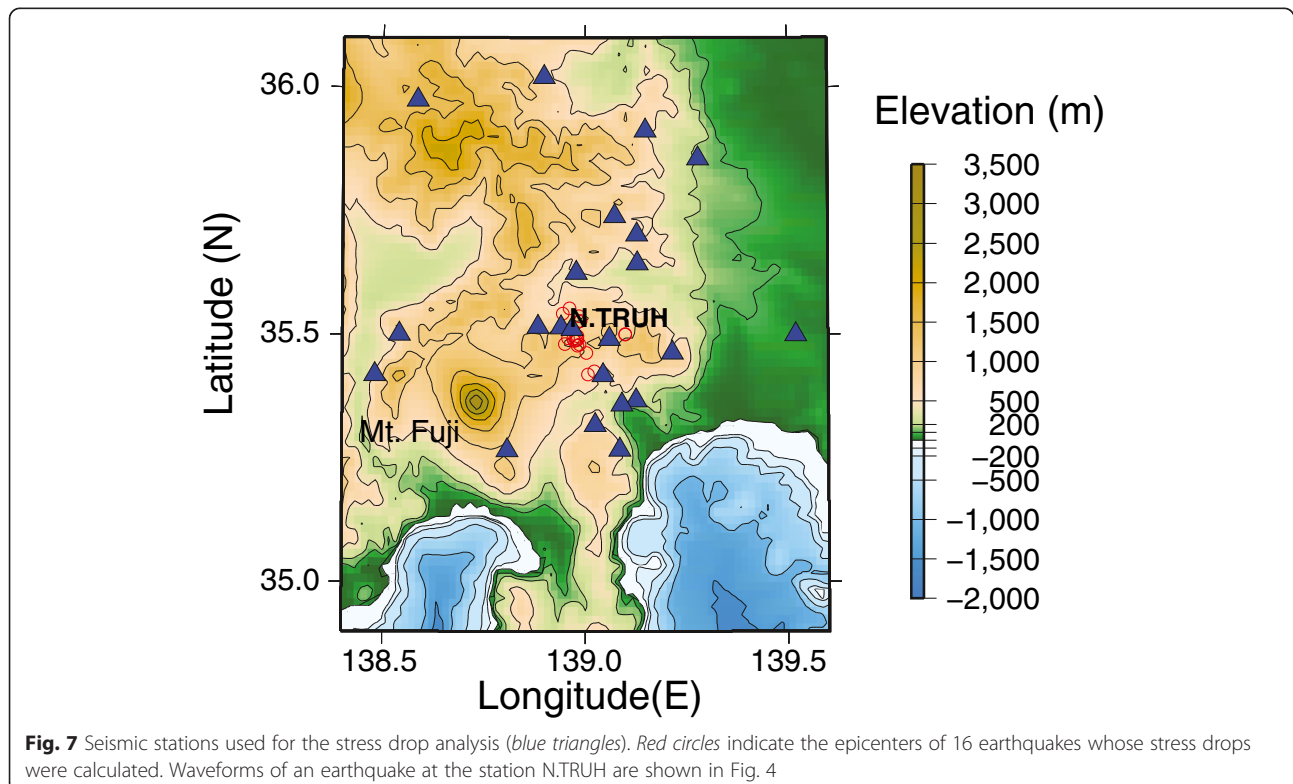




values of earthquakes that occurred in the same area before and after the activity. Average values of the stress drop are listed in Table 2 for the earthquakes during the 2012 cluster activity and the others before and after the activity. We carried out  $t$  tests for these values and confirmed that the temporal change was statistically significant within the 95 % confidence level. Figure 9 shows a map view of the estimated stress drops. We can clearly see that earthquakes with a larger stress drop took place in the vicinity of the cluster activity, thus suggesting that the temporal change in Fig. 8 was not an apparent change due to the spatial difference of hypocenters but an actual temporal change in stress drop.

One explanation for the observed temporal change of stress drop is that fluid could have raised the pore pressure and decreased the shear strength of the fault, and this triggered earthquakes with a small stress drop.

Figure 10 shows the calculated stress drops as a function of seismic moment. As the smaller earthquakes tended to have corner frequencies close to the Nyquist one, the results might include an artifact whereby the estimated stress drops for smaller earthquakes tended to decrease because of the limited frequency band availability. However, Fig. 10 clearly rules out this possibility in our study and suggests that the estimated small stress drops of the cluster activity did not come from an artifact due to the frequency band availability.



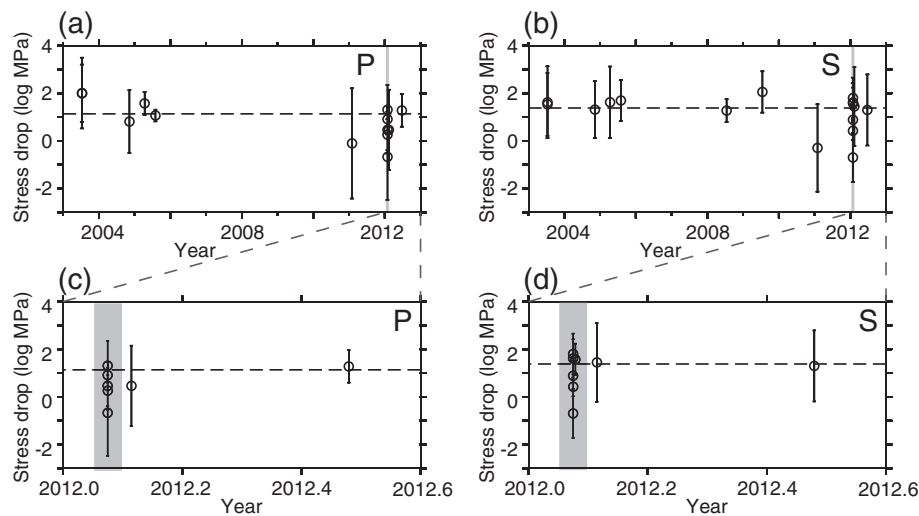


**Fig. 8** Estimated stress drops from (a) P and (b) S waves as a function of time. The horizontal broken line indicates the average stress drop of earthquakes that occurred before the cluster activity. Results after January 2012, which are shaded by the gray color in (a) and (b), are also shown in (c) and (d). Two earthquakes after the cluster activity had values of stress drop similar to those of earthquakes before the cluster activity

## Discussion

We found that the cluster activity in the Tanzawa Mountains during January 2012 showed hypocenter migration and the activity included earthquakes with a low stress drop. We first show that the migration was not an artificial one, but a real migration, and this was done through a numerical simulation; a discussion regarding the possibility of static/dynamic triggering is presented in “Hypocenter migration of the cluster activity”. We then conclude in “What caused the temporal change in the stress drop?” that the activity was due to a reduction of shear strength associated with a slow slip and an increase of pore pressure after discussing several candidate mechanisms. The spatiotemporal distribution of the stress drop also supports our conclusion, which is discussed in “Variety of estimated stress drops for earthquakes involved in the 2012 cluster activity”. Finally, we discuss the relationship of our results to the tectonics and velocity structure in the Tanzawa Mountains in “Relationship to the tectonics and velocity structure in the Tanzawa Mountains”.

## Hypocenter migration of the cluster activity

### Numerical test

As shown in Fig. 6, we characterized the hypocenter migration of the cluster activity in the Tanzawa Mountains at the end of January 2012. There was, however, the possibility that the observed migration was an artifact of the data. In order to investigate this possibility, we carried out a numerical test of the hypocenter migration.

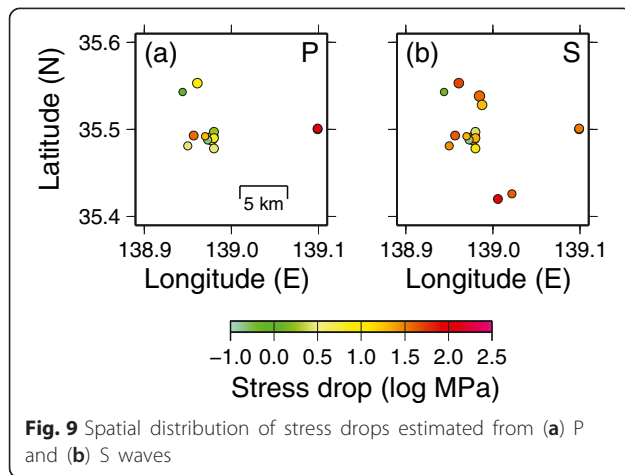
We relocated 218 earthquakes including 53 earthquakes with  $M \geq 2.0$  in the study area that had occurred within 50 h of the first one (M4.9) associated with the cluster activity. Taking this into account, we fixed the first earthquake at the center of a plane and plotted 52 synthetic hypocenters on the plane at random locations in space. We then calculated distances from the first earthquake to individual hypocenters and investigated whether we observed pseudo hypocenter migration. We set the origin times of the synthetic hypocenters to the same times as the actual ones.

For a quantitative analysis, we divided the 50 h into eight time windows; one from 0 to 0.1 h and seven time windows from 0.1 to 50 h with equal durations on a

**Table 2** Average values of the stress drop

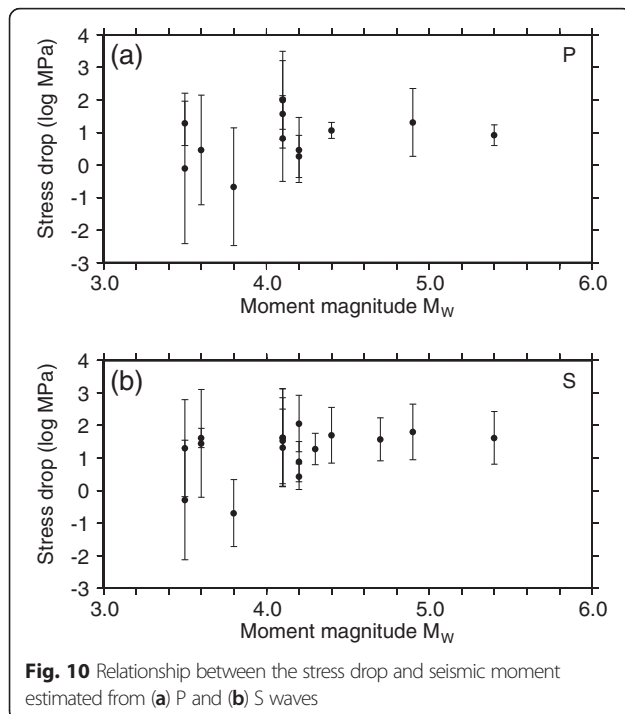
	Average values of stress drop (MPa) <sup>a</sup>	
The cluster activity in January, 2012	2.87 [5 eqs.]	8.61 [6 eqs.]
	(1.33–6.20)	(3.52–21.1)
Before and after the cluster activity	13.7 [8 eqs.]	22.8 [10 eqs.]
	(7.53–25.1)	(14.5–30.0)

<sup>a</sup>Values in the left and right columns show stress drops estimated by P and S waves, respectively. Values in brackets indicate the numbers of earthquakes used for calculating the average stress drops (see Table 1). Values in parentheses indicate the ranges for two standard errors



logarithmic scale. We then selected earthquakes with the longest distance in each time window and calculated the migration speed between the earthquakes in the successive time windows. As we had eight time windows, we obtained seven migration speeds. When we obtained more than four positive values out of the seven values, we defined it as “the migration was detected”. For the actual cluster activity in January 2012, all of the seven values were positive. We carried out this numerical test 50,000 times and investigated the frequency of false migrations.

Figure 11 shows two examples of origin times and the distances of 52 synthetic hypocenters. We observed apparent migrations as in Fig. 11b 1761 times



out of the 50,000 runs, which corresponds to 3.52 %. We concluded that the observed migration was statistically significant at the 95 % confidence level.

#### Migration or static/dynamic triggering

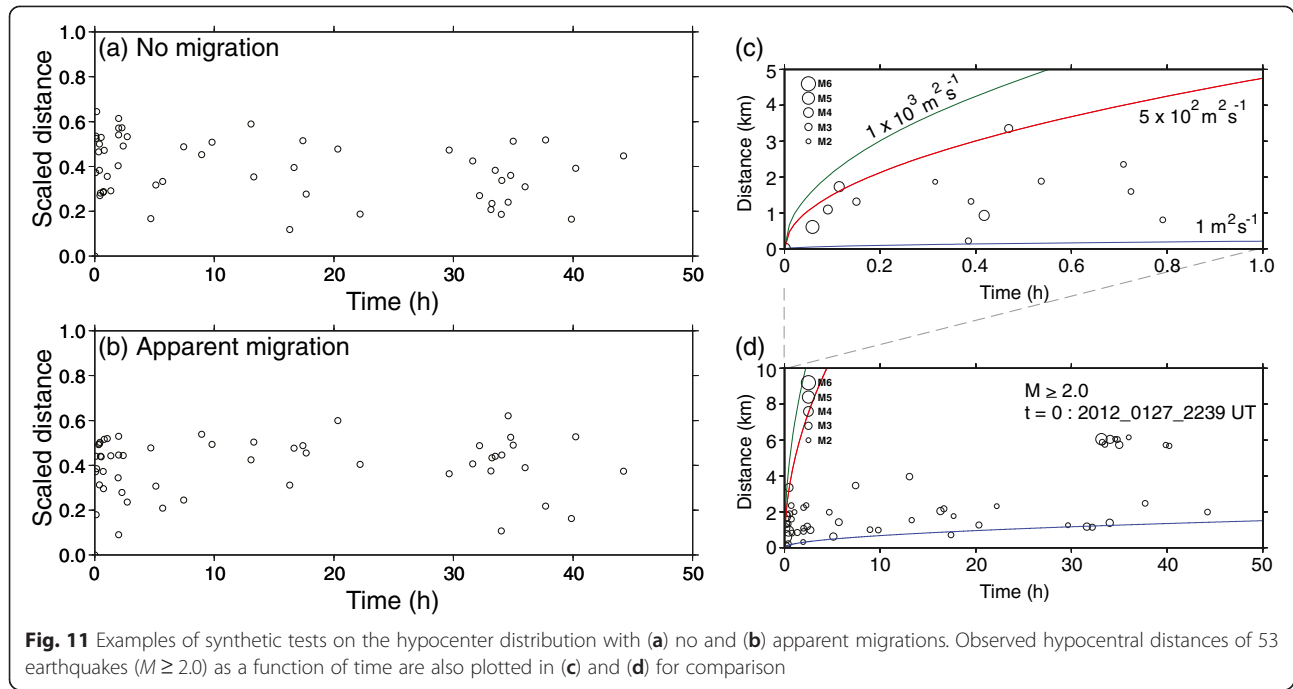
Although the synthetic simulation showed that the observed migration was not artificial, we will discuss here the possibility of static/dynamic triggering.

Figure 12 shows the relationship between the elapsed time and the distance from the first earthquake of the cluster activity, the same as Fig. 6, with estimated stress drops and orange vertical bars indicating the source radii of earthquakes obtained by the values of stress drops. For earthquakes without estimated values of stress drop, we assumed that the value was 8.61 MPa, which is the averaged value of the stress drop for earthquakes of the cluster activity.

When an earthquake takes place, shear stress will be concentrated at the edge of the fault plane, and then, successive earthquake activity will sometimes be triggered. Another possibility is that earthquakes can be dynamically triggered by the propagation of the seismic wave (e.g., Felzer and Brodsky 2006) and by indirect effects such as elevated pore pressure due to the passing Rayleigh wave (e.g., Hill et al. 1993). Figure 12 indicates that the cluster activity in January 2012 contained earthquakes far from fault planes of large ( $M \sim 5$ ) earthquakes compared to their source sizes. In addition, the activity showed continuous migration at least within the first 40 h. Although the observed migration would be difficult to explain only by the stress accumulation such as that caused by static triggering and direct dynamic triggering due to the passage of the seismic wave, our results suggest that the reduction of shear strength, including indirect dynamic triggering due to elevated pore pressure associated with the passage of seismic waves, played an important role in the cluster activity.

#### What caused the temporal change in the stress drop?

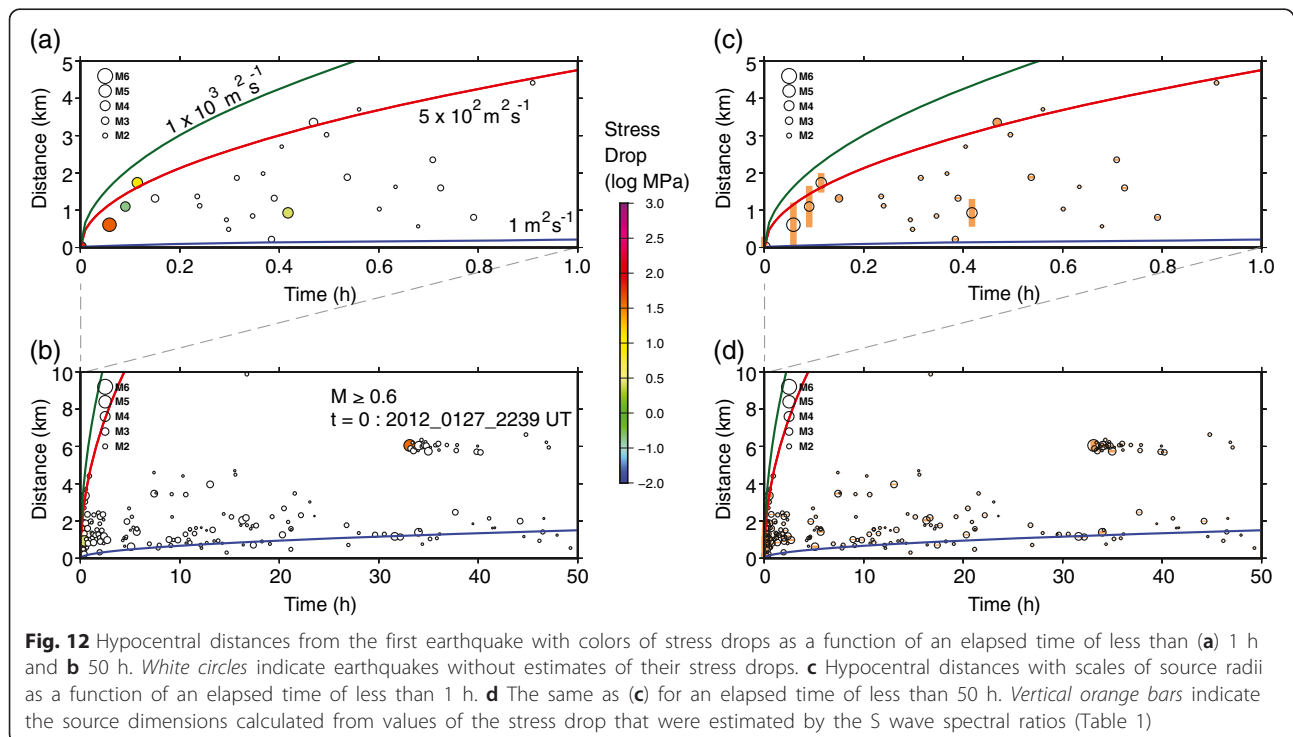
We found that three out of six earthquakes associated with the cluster activity in January 2012 had smaller values of stress drop (Table 1 and Fig. 8). We also found that the activity showed hypocenter migration consistent with a migration speed of deep non-volcanic tremors for the elapsed time of less than 1 h and with a speed of fluid-induced earthquakes for times later than 1 h (Figs. 6 and 12). These results are consistent with the decrease of shear strength due to fluid diffusion and a slow slip, for which fluid is significant for the generation (e.g., Suzuki and Yamashita 2010). However, it would be premature to insist at this moment that the activity was definitely triggered by fluid because there are other candidate mechanisms that could account for our results. Here, we discuss the other possibilities quantitatively, including changes



in the rupture speed, attenuation, and rigidity, and show that it is plausible that a slow slip and an increase of pore pressure due to fluid played the most important roles in the cluster activity for the first hour and the successive times, respectively.

#### Decrease of the shear strength

It has been reported that slow earthquakes including slow slips, deep episodic tremors, and low-frequency earthquakes are shear slips with long characteristic source durations that radiate less seismic energy (e.g.,





Hirose et al. 1999; Ito et al. 2006; Obara 2002); this suggests that they have small stress drops. Ide et al. (2007) showed that these slow earthquakes are different manifestations of the same phenomena and follow a unified scaling relationship. Although the rate- and state-dependent friction law can account for the propagation of a slow slip without fluid (Liu and Rice 2005), it would be natural that slow slips are associated with fluid, as suggested by the existence of fluid on the plate interface (Kato et al. 2010; Kodaira et al. 2004; Shelly et al. 2006) where tremors and slow slip events are observed.

Kato and Obara (2014) observed migration of aftershocks following the 2007 Noto-Hanto earthquake. They concluded that the expansion of the aftershock area was driven mainly by aseismic afterslip. Taking these previous studies into account, the most plausible possibility for the observed migration and small stress drops during the 2012 cluster activity in the Tanzawa Mountains is that they were triggered by a slow slip associated with fluid activity that produced a decrease in the shear strength. This hypothesis is also supported quantitatively by the diffusivity for the first hour of the cluster activity. As briefly discussed in “Hypocenter migration”, we obtained a diffusivity  $D$  of  $5.0 \times 10^2 \text{ m}^2 \text{ s}^{-1}$  for the first hour of the cluster activity. This value is consistent with that for the migration of non-volcanic deep tremors (Ide 2010), which suggests that a slow slip on the extension for fault planes of earthquakes with an elapsed time of less than 0.1 h may have played an important role in the cluster activity for the first hour. Unfortunately, the spatial scale of the cluster activity indicates that the slow slip had a dimension of a few kilometers at the depth of 20 km, thus suggesting that it would be difficult to detect at the surface.

On the other hand, decreased effective normal stress due to fluid without the contribution of a slow slip likely played the most important role for the activity with elapsed times larger than 1 h. Importantly, the data showed that the observed speed of migration was consistent with the speed of fluid diffusion and fluid-induced earthquakes.

Talwani et al. (2007) compiled studies on the seismogenic permeability of triggered earthquakes associated with reservoir water level fluctuations, injection of high-pressure fluids in deep boreholes, and seasonal groundwater recharges. They concluded that the value of diffusivity  $D$ , which is defined as shown in Eq. (8), ranged from 0.03 to  $3 \text{ m}^2 \text{ s}^{-1}$ . This is consistent with the migration speed of the cluster activity in the Tanzawa Mountains during January 2012 for the elapsed times that were larger than 1 h. Note that the value is two orders of magnitudes smaller than the migration speed of non-volcanic deep tremors.

The discussion above suggests that the cluster activity was triggered by a decrease in the shear strength on the fault planes. For the elapsed time of less than 1 h, a slow slip, rather than only fluid diffusion, likely played an important role in the cluster activity. The successive activity could have been triggered mainly by the decrease of the shear strength due to the increase of the pore pressure associated with the fluid diffusion. Although the above scenario is supported quantitatively by the diffusivity, indirect dynamic triggering may have also played an important role in the reduction of the shear strength, such as through elevated pore pressures and successive fluid diffusion due to Rayleigh waves of larger earthquakes in the 2012 cluster activity; this could have resulted in an overestimated diffusivity at the early stage. Even if this was the case, our conclusion does not change that the reduction of shear strength played the most important role in the cluster activity.

#### **Rupture speed**

As noted in “Stress drop analysis”, stress drop for a circular fault can be estimated from Eq. (1). Since actual fault sizes of small earthquakes are unknown in most cases, we usually estimate the fault dimension from the observed corner frequency. Models of Brune (1970) and Madariaga (1976) are commonly used (see Eqs. (2) and (3)). The largest difference of the two models is the assumed rupture speed, whereby the former uses the infinite rupture speed and the latter employs 90 % of the shear wave velocity. An estimated value of stress drop is proportional to an observed corner frequency to the third power for both models.

Here, we consider a situation where two earthquakes X and Y have the same stress drops but the rupture speed of earthquake X is half of the value of earthquake Y. As the stress drop analysis from the observed corner frequencies usually assumes that the rupture speeds of earthquakes are the same, the fault dimension of earthquake X is overestimated, thus resulting in an estimated stress drop for earthquake X that is an order of magnitude smaller than the actual one and the value of earthquake Y. This shows that if the rupture speeds of earthquakes associated with the cluster activity were half of the speeds of the other earthquakes, calculated values of the stress drop could have been an order of magnitude smaller than the actual values because of the overestimated fault size.

We may not be able to strongly deny the possibility that earthquakes involved in the cluster activity had extremely slow rupture speeds and the observed temporal change in the stress drop, which changed by an order of magnitude, was an artifact. This possibility, however, is very unlikely because the rupture speeds of small earthquakes would not be extremely slow and they would not vary significantly (e.g., Yamada et al. 2005).

### ***Slip velocity on a fault***

It is well known that dynamic friction is strongly related to the slip velocity around  $1 \text{ m s}^{-1}$  (Di Toro et al. 2011), which is a common value for the slip rate of an earthquake rupture. If earthquakes of the cluster activity had a slow slip velocity, the dynamic stress level would have been high during the rupture and observed small stress drops could be explained even though there was no temporal change in the shear strength. As the hypocenters of the earthquakes of which the stress drops were analyzed were close to each other, this possibility suggests that earthquakes involved in the cluster activity had small slip rates under no difference in conditions of stress and friction. This is unlikely to be the case.

### ***Strong spatial heterogeneity of frictional parameters***

If there were extremely strong, fine-scale spatial heterogeneities of the frictional parameters in the source area of the cluster activity, then an apparent temporal change of the stress drop might have been observed because such heterogeneity would have been neglected when calculating the seismic moments of earthquakes. Judging from the stability of the estimated stress drop before and after the cluster activity (Fig. 8) and spatial distribution of stress drops as shown in Fig. 9, this would be quite unlikely to be the main reason that accounts for our results; this was also discussed in “Small stress drop”.

### ***Temporal change in the rigidity and attenuation***

To account for our results in terms of the temporal change of rigidity, it should have become 10 times larger only during the cluster activity and returned to the original value immediately after the activity. This would have been impossible.

Another possibility is that the observed temporal change of stress drop was due to the temporal change of attenuation. If this was the case, attenuation should have changed dramatically over the whole ray path and this would have decreased the observed corner frequency by half. In addition, the changed attenuation should have come back to the original one immediately after the cluster activity. This was also hardly the case.

As a result, it is most plausible that the decrease of the shear strength due to fluid associated with a slow slip played the most important role in the cluster activity. Importantly, the increase of pore pressure can quantitatively account for both the observed temporal change in the stress drop and the migration of the hypocenters.

### ***Variety of estimated stress drops for earthquakes involved in the 2012 cluster activity***

Although the cluster activity included earthquakes with a small stress drop, not all the earthquakes had smaller values compared to the earthquakes before and after the

cluster activity in January 2012 (Fig. 8). Referring to Table 1, earthquakes during the cluster activity with magnitudes of 4.9, 5.4, and 4.7 had values of stress drop similar to those of earthquakes that occurred before the cluster activity. Figures 6 and 12 suggest that these three earthquakes occurred at the migration front of the cluster activity. These results can be explained as follows.

Earthquake rupture initiates when and where the shear stress is equal to the shear strength, and it will be mainly controlled by two effects, namely, the stress accumulation and the strength reduction. The former effect will be dominant for most earthquakes, but some earthquakes are triggered by the latter effect. As the stress drop represents the difference of shear stress before and after the earthquake and is a proxy of the difference between the shear strength and the dynamic stress level (Yamada et al. 2010), earthquakes caused by the latter effect will have smaller stress drops. Here, we assume that the increase of pore pressure triggers an earthquake at the migration front of the fluid. The rupture can expand because of the stress concentration at the crack tip in the direction where the pore pressure has not been raised. In this case, the shear strength has not been reduced by the increased pore pressure on most parts of the fault plane. Because the stress drop of the earthquake is calculated as a representative value over the fault plane, the estimated stress drop could almost be the same as if there is no reduction in the shear strength. On the other hand, an earthquake that is triggered in an area with abundant fluid around the source area will show a smaller value of stress drop because the shear strength will be decreased anywhere on the fault plane by the increase of pore pressure. The three earthquakes with magnitudes of 4.9, 5.4, and 4.7 that occurred at the migration front of the cluster activity could have been triggered under the first situation explained above as they have values of stress drop similar to those of earthquakes that occurred before the cluster activity.

An earthquake on January 30, 2011 that occurred a year before the 2012 cluster activity also had a small stress drop. Though the reason is unclear, one possibility would be that the estimated stress drop of the earthquake was the least robust among the analyzed earthquakes because the earthquake had the largest standard deviation of estimated stress drop, which was calculated from individual corner frequencies of waveforms observed by the individual components of stations.

Stress drops of small earthquakes reflect the difference of the shear strength and the dynamic stress level. As the slip velocity of earthquakes, except for slow slips, is on the order of  $1 \text{ m s}^{-1}$ , the dynamic stress level could also be of the same order of magnitude (Di Toro et al. 2011). This suggests that the spatial distribution of stress drops can give us the distribution of the shear strength

as mentioned by Yamada et al. (2010). Precise analysis of the stress drop can therefore provide important information on the earthquake dynamics and the physical properties of seismogenic regions.

#### Relationship to the tectonics and velocity structure in the Tanzawa Mountains

As mentioned in the “Background”, several tectonic faults have developed in response to the collision in the Tanzawa Mountains. The cluster activity of 2012 seems to have occurred on a plane dipping to the SE with a NE-SW strike (Fig. 5), and the source area was located in the deeper extension of the SE-dipping Sone Hills faults (Arai et al. 2013). This is also consistent with the tectonic characteristics of this region.

Nakamichi et al. (2007) determined the three-dimensional velocity structures of Mt. Fuji and the South Fossa Magna, including the Tanzawa Mountains. Their results show that the  $V_p/V_s$  ratio is high in the source region of the cluster activity, but velocities of P and S waves are not low. It is worth noting that their results for velocity are close to the value of gabbro, which includes little hydrous minerals. Aizawa et al. (2004) analyzed the resistivity of the region. They found areas with a low resistivity south-west of and beneath Mt. Fuji, but a notable low resistivity area was not detected beneath the Tanzawa Mountains. These results suggest that there would have been little fluid in the source area of the cluster activity. Arai et al. (2014) reached a similar conclusion from tectonic and mineralogical analyses.

Our results are consistent with these previous studies. If there are a lot of cracks filled with fluid in the source area of the cluster activity, earthquakes in the area should have stably small values of stress drop over time. However, Fig. 8 shows that earthquakes before and after the cluster activity had consistent values of stress drop and only the cluster activity included earthquakes with smaller stress drops. This result suggests that the source region was under a dry condition and a sudden increase of pore pressure with a slow slip may have caused the cluster activity.

If the increase of pore pressure really took place, fluid incursion would have preceded the event. Although the origin of fluid is unclear, one possibility is that there is a little fluid in a closed system beneath the Tanzawa Mountains that is undetectable by structural observations. Abe et al. (2011) found a velocity boundary dipping in the south-east direction from the source region of the cluster activity to the Philippine Sea plate by stacking scattered teleseismic waves. Hypocenters of the cluster activity seem to lie on this boundary. This boundary might provide a way for episodic fluid incursion, though there would not have been abundant fluid steadily in the source area of the cluster activity as

suggested by our results as well as those of the velocity tomography and resistivity studies.

#### Conclusions

A cluster of earthquake activity took place beneath the Tanzawa Mountains at a depth of 20 km during the end of January 2012. We relocated the hypocenters by using the double-difference method and found their migration away from the first earthquake of the cluster activity. The migration was consistent with fluid diffusion and had a similar speed to that of non-volcanic tremors during the first hour and to activity induced by water-injection experiments during the successive times. We then analyzed the stress drops of 16 earthquakes of M3.5 and greater that occurred from July 2003 to June 2012 in the area of the cluster activity. Earthquakes that occurred before and after the cluster activity had typical values of stress drop. This is consistent with structural studies indicating the existence of little fluid in the region. On the other hand, the cluster activity included earthquakes with significantly small stress drops. A hypothesis that the cluster activity was triggered by fluid, probably associated with a slow slip for the first hour, was put forward to explain both the migration of hypocenters and small stress drops of the cluster activity. This hypothesis was also supported by the fact that earthquakes before and after the cluster activity had similar values of stress drop, thus suggesting that the activity was triggered by a different mechanism from the other earthquakes in the same region. Although the origin of fluid is unclear, there may be a little fluid in a closed system beneath the Tanzawa Mountains that is undetectable by structural observations.

#### Competing interests

The authors declare that they have no competing interests.

#### Authors' contributions

TY carried out the stress drop analysis and numerical test for the hypocenter migration and wrote the manuscript. YY carried out the hypocenter relocation. YY, TT, and RA helped to interpret the results. All the authors read and approved the final manuscript.

#### Acknowledgements

The authors are grateful to Editor Takuto Maeda, Editor-in-Chief Yasuo Ogawa, and two anonymous reviewers for their comments and suggestions that improved the manuscript. We used waveforms from stations that were part of Hi-net (NIED), the Hot Spring Research Institute of Kanagawa Prefecture, Univ. of Tokyo, and JMA, as well as the seismograph network called MeSO-net (Hirata et al. 2009; Sakai and Hirata 2009), which was developed under the “Special Project for Earthquake Disaster Mitigation in the Tokyo Metropolitan Area” in 2007. We also used arrival times of P and S waves determined by JMA. Figures were created with Genetic Mapping Tool software (Wessel and Smith 1991).

#### Author details

<sup>1</sup>Department of Earth Sciences, Faculty of Science, Ibaraki University, Mito, Ibaraki, Japan. <sup>2</sup>Hot Springs Research Institute of Kanagawa Prefecture, Odawara, Kanagawa, Japan. <sup>3</sup>Earthquake and Volcano Research Center, Graduate School of Environmental Studies, Nagoya University, Nagoya, Aichi, Japan. <sup>4</sup>Research and Development Center for Earthquake and Tsunami, Japan Agency for Marine-Earth Science and Technology, Yokohama, Kanagawa, Japan.

Received: 3 June 2015 Accepted: 15 October 2015

Published online: 28 October 2015

## References

- Abe S, Sato H, Kurashimo E, Hirata N, Iwasaki T, Kawanaka T (2011) Hybrid prestack migration of scattered teleseismic waves and local earthquake sequences for the imaging of source fault and subducting slab, Abstr AGU Fall Meeting, T14A-04
- Abercrombie RE (1995) Earthquake source scaling relationships from  $-1$  to  $5 M_L$  using seismograms recorded at 2.5-km depth. *J Geophys Res* 100:24015–24036
- Aizawa K, Yoshimura R, Oshiman N (2004) Splitting of the Philippine Sea plate and a magma chamber beneath Mt. Fuji. *Geophys Res Lett* 31:L09603. doi:10.1029/2004GL019477
- Allmann BP, Shearer PM (2007) Spatial and temporal stress drop variations in small earthquakes near Parkfield, California. *J Geophys Res* 112:B04305. doi:10.1029/2006JB004395
- Ando R, Imanishi K (2011) Possibility of  $M_W$  9.0 mainshock triggered by diffusional propagation of after-slip from  $M_W$  7.3 foreshock. *Earth Planets Space* 63:767–771. doi:10.5047/eps.2011.05.016
- Arai R, Iwasaki T (2014) Crustal structure in the northwestern part of the Izu collision zone in central Japan. *Earth Planets Space* 66:21. doi:10.1186/1880-5981-66-21
- Arai R, Iwasaki T (2015) Transition from collision to subduction and its relation to slab seismicity and plate coupling. *Earth Planets Space* 67:76. doi:10.1186/s40623-015-0247-6
- Arai R, Iwasaki T, Sato H, Abe S, Hirata N (2013) Crustal structure of the Izu collision zone in central Japan from seismic refraction data. *J Geophys Res* 118:6258–6268. doi:10.1002/2013JB010532
- Arai R, Iwasaki T, Sato H, Abe S, Hirata N (2014) Contrasting subduction structures within the Philippine Sea plate: Hydrous oceanic crust and anhydrous volcanic arc crust. *Geochem Geophys Geosyst* 15:1977–1990. doi:10.1002/2014GC005321
- Biot MA (1962) Mechanics of deformation and acoustic propagation in porous media. *J Appl Phys* 33:1482–1498
- Boatwright J (1978) Detailed spectral analysis of two small New York State earthquakes. *Bull Seismol Soc Am* 68:1131–1177
- Brune JN (1970) Tectonic stress and the spectra of seismic shear waves from earthquakes. *J Geophys Res* 75:4997–5009 (Correction, *J Geophys Res*, 76:5002, 1971)
- Di Toro G, Han R, Hirose T, De Paola N, Nielsen S, Mizoguchi K, Ferri F, Cocco M, Shimamoto T (2011) Fault lubrication during earthquakes. *Nature* 471:494–498. doi:10.1038/nature09838
- Dieterich J (1994) A constitutive law for rate of earthquake production and its application to earthquake clustering. *J Geophys Res* 99(B2):2601–2618
- Eshelby JD (1957) The determination of the elastic field of an ellipsoidal inclusion and related problems. *Proc R Soc London Ser A* 241:376–396
- Felzer KR, Brodsky BB (2006) Decay of aftershock density with distance indicates triggering by dynamic stress. *Nature* 441:735–738. doi:10.1038/nature04799
- Goertz-Allmann BP, Goertz A, Wiemer S (2011) Stress drop variations of induced earthquakes at the Basel geothermal site. *Geophys Res Lett* 38:L09308. doi:10.1029/2011GL047498
- Hanks TC, Kanamori H (1979) A moment magnitude scale. *J Geophys Res* 84(B5):2348–2350
- Hill DP, Reasenber PA, Michael A, Arabaz WJ, Beroza G, Brumbaugh D, Brune JN, Castro R, Davis S, dePollo D, Ellsworth WL, Gombert J, Harmsen S, House L, Jackson SM, Johnston MJS, Jones L, Keller R, Malone S, Munguia L, Nava S, Pechmann JC, Sanford A, Simpson RW, Smith RB, Stark M, Stickney M, Vidal A, Walter S, Wong V, Zollweg J (1993) Seismicity remotely triggered by the magnitude 7.3 Landers, California, earthquake. *Science* 260:1617–1623
- Hiraga S (1987) Seismicity of Hakone volcano and its adjacent area. *Bull Hot Springs Res Inst Kanagawa Pref* 18:125 (in Japanese)
- Hirata N, Sakai S, Sato H, Satake K, Koketsu K (2009) An outline of the Special Project for Earthquake Disaster Mitigation in the Tokyo Metropolitan Area - Subproject I: characterization of the plate structure and source faults in and around the Tokyo Metropolitan area. *Bull Earthq Res Inst Univ Tokyo* 84:41–56 (in Japanese)
- Hirose H, Hirahara K, Kimata F, Fujii N, Miyazaki S (1999) A slow thrust slip event following the two 1996 Hyuganada earthquakes beneath the Bungo Channel, southwest Japan. *Geophys Res Lett* 26:3237–3240
- Hirose F, Nakajima J, Hasegawa A (2008a) Three-dimensional seismic velocity structure and configuration of the Philippine Sea slab in southwestern Japan estimated by double-difference tomography. *J Geophys Res* 113:B09315. doi:10.1029/2007JB005274
- Hirose F, Nakajima J, Hasegawa A (2008b) Three-dimensional velocity structure and configuration of the Philippine Sea slab beneath Kanto District, Central Japan, estimated by double-difference tomography. *Zisin Ser 2*(60):123–138 (in Japanese with English abstract)
- Hirose F, Miyaoka K, Hayashimoto N, Yamazaki T, Nakamura M (2011) Outline of the 2011 off the Pacific coast of Tohoku Earthquake ( $M_W$  9.0) -Seismicity: foreshocks, mainshock, aftershocks, and induced activity-. *Earth Planets Space* 63:513–518. doi:10.5047/eps.2011.05.019
- Ide S (2010) Striations, duration, migration and tidal response in deep tremor. *Nature* 466:356–360. doi:10.1038/nature09251
- Ide S, Beroza GC, Shelly DR, Uchide T (2007) A scaling law for slow earthquakes. *Nature* 447:76–79. doi:10.1038/nature05780
- Imanishi K, Ellsworth WL (2006) Source scaling relationships of microearthquakes at Parkfield, CA, determined using the SAFOD pilot hole seismic array. In: Abercrombie RE, McGarr A, Kanamori H, Di Toro G (eds) *Earthquakes: radiated energy and the physics of earthquake faulting*, vol 170, *Geophys Monogr Ser.* AGU, Washington D.C., pp 81–90
- Imanishi K, Takeo M, Ellsworth WL, Ito H, Matsuzawa T, Kuwahara Y, Iio Y, Horiuchi S, Ohmi S (2004) Source parameters and rupture velocities of microearthquakes in Western Nagano, Japan, determined using stopping phases. *Bull Seismol Soc Am* 94:1762–1780. doi:10.1785/012003085
- Ishii M, Shearer PM, Houston H, Vidale J (2005) Extent, duration and speed of the 2004 Sumatra-Andaman earthquake imaged by the Hi-Net array. *Nature* 435:933–936. doi:10.1038/nature03675
- Ito Y, Obara K, Shiomi K, Sekine S, Hirose H (2006) Slow earthquakes coincident with episodic tremors and slow slip events. *Science* 265:503–506
- Kanamori H, Anderson DL (1975) Theoretical basis of some empirical relations in seismology. *Bull Seismol Soc Am* 65:1073–1095
- Kato A, Obara K (2014) Step-like migration of early aftershocks following the 2007  $M_W$  6.7 Noto-Hanto earthquake, Japan. *Geophys Res Lett* 41:3864–3869. doi:10.1002/2014GL060427
- Kato A, Iidaka T, Ikuta R, Yoshida Y, Katsumata K, Iwasaki T, Sakai S, Thurber C, Tsumura N, Yamaoka K, Watanabe T, Kunitomo T, Yamazaki F, Okubo M, Suzuki S, Hirata N (2010) Variations of fluid pressure within the subducting oceanic crust and slow earthquakes. *Geophys Res Lett* 37:L14310. doi:10.1029/2010GL043723
- Kato A, Obara K, Igarashi T, Tsuruoka H, Nakagawa S, Hirata N (2012) Propagation of slow slip leading up to the 2011  $M_W$  9.0 Tohoku-Oki earthquake. *Science* 335:705–708. doi:10.1126/science.1215141
- Kobayashi R, Koketsu K (2005) Source process of the 1923 Kanto earthquake inferred from historical geodetic, teleseismic, and strong motion data. *Earth Planets Space* 57:261–270
- Kodaira S, Iidaka T, Kato A, Park J, Iwasaki T, Kaneda Y (2004) High pore fluid pressure may cause silent slip in the Nankai trough. *Science* 304:1295–1298. doi:10.1126/science.1096535
- Liu Y, Rice JR (2005) Aseismic slip transients emerge spontaneously in three-dimensional rate and state modeling of subduction earthquake sequences. *J Geophys Res* 110:B08307. doi:10.1029/2004JB003424
- Madariaga R (1976) Dynamics of an expanding circular fault. *Bull Seismol Soc Am* 66:639–666
- Nakajima J, Hirose F, Hasegawa A (2009) Seismotectonics beneath the Tokyo metropolitan area, Japan: effect of slab-slab contact and overlap on seismicity. *J Geophys Res* 114:B08309. doi:10.1029/2008JB006101
- Nakamichi H, Watanabe H, Ohminato T (2007) Three-dimensional velocity structures of Mount Fuji and the South Fossa Magna, central Japan. *J Geophys Res* 112:B03310. doi:10.1029/2005JB004161
- Naoki M, Nakatani M, Otsuki K, Yabe Y, Kgarume T, Murakami O, Masakale T, Ribeiro L, Ward A, Moriya H, Kawakata H, Durrheim R, Ogasawara H (2015) Steady activity of microfractures on geological faults loaded by mining stress. *Tectonophysics* 649:100–114
- Obara K (2002) Nonvolcanic deep tremor associated with subduction in southwest Japan. *Science* 296:1679–1681
- Oth A (2013) On the characteristics of earthquake stress release variations in Japan. *Earth Planet Sci Lett* 377–378:132–141. doi:10.1016/j.epsl.2013.06.037
- Prieto GA, Shearer PM, Vernon FL, Klib D (2004) Earthquake source scaling and self-similarity estimation from stacking P and S spectra. *J Geophys Res* 109:B08310. doi:10.1029/2004JB003084



- Research Group for Active Faults of Japan (1991) Active faults in Japan, sheet maps and inventories, rev ed, 437. Univ of Tokyo Press, Tokyo
- Sakai S, Hirata N (2009) Distribution of the Metropolitan Seismic Observation network. *Bull Earthq Res Inst Univ Tokyo* 84:57–70 (in Japanese)
- Seno T, Stein S, Gripp AE (1993) A model for the motion of the Philippine Sea Plate consistent with NUVEL-1 and geological data. *J Geophys Res* 98:17941–17948. doi:10.1029/93JB00782
- Shapiro SA, Huenges E, Borm G (1997) Estimating the crust permeability from fluid-injection-induced seismic emission at the KTB site. *Geophys J Int* 131:F15–F18
- Shearer PM (1997) Improving local earthquake locations using the L1 norm and waveform cross correlation: application to the Whittier Narrows, California, aftershock sequence. *J Geophys Res* 102:8269–8283
- Shelly DR, Beroza GC, Ide S, Nakamura S (2006) Low-frequency earthquakes in Shikoku, Japan, and their relationship to episodic tremor and slip. *Nature* 442:188–191. doi:10.1038/nature04931
- Shelly DR, Beroza GC, Ide S (2007) Non-volcanic tremor and low-frequency earthquake swarms. *Nature* 446:305–307. doi:10.1038/nature05666
- Suzuki T, Yamashita T (2010) Nondimensional control parameters governing the behavior of one-dimensional fault slip: effects of shear heating, inelastic pore creation, and fluid flow. *J Geophys Res* 115:B02303. doi:10.1029/2009JB006557
- Tadokoro K, Ando M, Nishigami K (2000) Induced earthquakes accompanying the water injection experiment at the Nojima fault zone, Japan: seismicity and its migration. *J Geophys Res* 105(B3):6089–6104
- Talwani P, Chen L, Gahalaut K (2007) Seismogenic permeability,  $k_s$ . *J Geophys Res* 112:B07309. doi:10.1029/2006JB004665
- Terakawa T, Matsu'ura M (2010) The 3-D tectonic stress fields in and around Japan inverted from centroid moment tensor data of seismic events. *Tectonics* 29:TC6008. doi:10.1029/2009TC002626
- Toda S, Stein RS, Sagiya T (2002) Evidence from the AD 2000 Izu islands earthquake swarm that stressing rate governs seismicity. *Nature* 419:58–61. doi:10.1038/nature00997
- Tomic J, Abercrombie RE, do Nascimento AF (2009) Source parameters and rupture velocity of small  $M \leq 2.1$  reservoir induced earthquakes. *Geophys J Int* 179:1013–1023
- Wald DJ, Heaton TH (1994) Spatial and temporal distribution of slip for the 1992 Landers, California, earthquake. *Bull Seismol Soc Am* 84:668–691
- Waldhauser F, Ellsworth WL (2000) A double-difference earthquake location algorithm: method and application to the North Hayward fault. *Bull Seismol Soc Am* 90:1352–1368
- Wei D, Seno T (1998) Determination of the Amurian plate motion. In: Flower MFJ, Chung SL, Lo CH, Lee TY (eds) *Mantle dynamics and plate interactions in East Asia*, vol 27, *Geodynamics Ser.* AGU, Washington D.C, pp 337–346
- Wessel P, Smith W (1991) Free software helps map and display data. *EOS Trans AGU* 72(441):445–446
- Yamada T, Mori JJ, Ide S, Kawakata H, Iio Y, Ogasawara H (2005) Radiation efficiency and apparent stress of small earthquakes in a South African gold mine. *J Geophys Res* 110:B01305. doi:10.1029/2004JB003221
- Yamada T, Mori JJ, Ide S, Abercrombie RE, Kawakata H, Nakatani M, Iio Y, Ogasawara H (2007) Stress drops and radiated seismic energies of microearthquakes in a South African gold mine. *J Geophys Res* 112:B03305. doi:10.1029/2006JB004553
- Yamada T, Okubo PG, Wolfe CJ (2010) Kiholo Bay, Hawai'i, earthquake sequence of 2006: relationship of the main shock slip with locations and source parameters of aftershocks. *J Geophys Res* 115:B08304. doi:10.1029/2009JB006657
- Yoshimitsu N, Kawakata H, Takahashi N (2014) Magnitude  $-7$  level earthquakes: a new lower limit of self-similarity in seismic scaling relationships. *Geophys Res Lett* 41:4495–4502. doi:10.1002/2014GL060306
- Yukutake Y, Takeda T, Honda R, Yoshida A (2012) Seismotectonics in the Tanzawa Mountains area in the Izu-Honshu collision zone of central Japan, as revealed by precisely determined hypocenters and focal mechanisms. *Earth Planets Space* 64:269–277

**Submit your manuscript to a SpringerOpen<sup>®</sup> journal and benefit from:**

- Convenient online submission
- Rigorous peer review
- Immediate publication on acceptance
- Open access: articles freely available online
- High visibility within the field
- Retaining the copyright to your article

---

Submit your next manuscript at ► [springeropen.com](http://springeropen.com)